

The Evolution of Pyritic and Organic Sulfur from Pulverized Coal Particles during Combustion

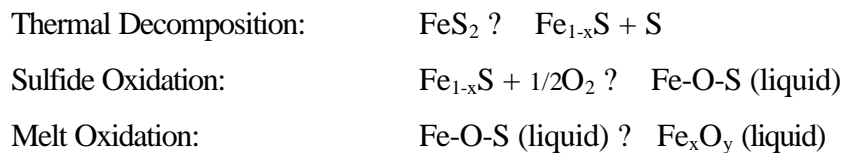
Kevin Davis, Adam Dissel, and James Valentine

Reaction Engineering International
Salt Lake City, UT

INTRODUCTION

Background

Sulfur associated with coal is comprised of both organic and inorganic components. In North America the inorganic phase is predominately pyritic and can exist both as distinct particles (excluded) and within the coal matrix (included). The fraction of the initial excluded and included pyrite that is conveyed into a particular boiler varies widely and is known to be highly dependent upon the fineness to which the coal is ground [Bryers and Taylor, 1976] and the particulars of the mill used. Over the past 15 years a number of studies focusing on the decomposition and subsequent oxidation of excluded pyrite have been performed [Asaki et al., 1985; Groves et al., 1987; Srinivasachar and Boni, 1989; Huffman et al., 1989; ten Brink et al., 1996]. This body of work has resulted in a mechanistic description for excluded pyrite that, in simple terms, can be illustrated as follows:



Thermal decomposition is heat transfer limited and occurs along a thermal front that propagates inward and is complete on the order of 10msec. The product of this decomposition process is a sulfide such as pyrrhotite ($\text{Fe}_{0.877}\text{S}$) or troilite ($\text{Fe}_{1.0}\text{S}$). In the presence of oxygen, the Fe_{1-x}S is oxidized in a manner that studies indicate is limited by boundary layer diffusion. As an outer layer of FeO begins to form, the exothermic nature of this reaction begins to melt the particle and Fe-O-S liquid forms. At least initially, this liquid oxidizes at a rate that can be further limited by diffusion of oxygen through the melt. As the particle temperature continues to increase, there is evidence to suggest that this limitation will quickly diminish and, again, the reaction proceeds limited only by gas-phase diffusion. At higher temperatures and more reducing conditions, wustite (FeO) and magnetite (Fe_3O_4) are the dominant iron oxidation products. At lower temperatures and more oxidizing conditions, magnetite and hematite (Fe_2O_3) dominate. In this work we are primarily interested in the high temperature oxidation processes.

Previous work at Reaction Engineering International (REI) [Davis et al., 1999; Valentine et al., 2000] has drawn upon these earlier investigations to develop a computational approach incorporating these physics into a CFD tool that has proven valuable for both utility and smelting [Adams et al., 1999]

applications. However, recent developments have required that more complete models of sulfur evolution from pulverized coal be developed.

Motivation

Until recently, waterwall corrosion in North American coal-fired boilers was uncommon and relatively mild. However, the introduction of combustion modifications to reduce in-furnace NO_x formation has led to notable increases in the frequency and severity of waterwall wastage [Jones, 1997]. As the extent of air staging is increased to satisfy more stringent restrictions on NO_x emissions, there is justifiable concern that this will result in elevated rates of high temperature corrosion and waterwall wastage. The most damaging impact has been to supercritical pulverized-coal-fired units, but even operators of less susceptible units must now consider the possibility of higher rates of tube metal loss at elevations near and below over-fire air ports. REI has worked with EPRI and the Department of Energy to improve predictive capabilities and provide solutions for furnace wall wastage for a wide range of coal-fired furnaces.

Utilities with low NO_x firing systems would like to quantify the increased potential for water wall wastage when evaluating strategies involving low NO_x combustion modifications. Unscheduled outages and the replacement of water wall sections are expensive, as are preventative measures such as weld overlays or spray coatings. Minor modifications to operating conditions or firing systems can be cost effective but a decision making tool is needed to quantify the effect of these modifications on wastage rates. Thus, there is a need for reliable prediction of water wall corrosion rates.

CFD TOOLS FOR THE ANALYSIS OF CORROSION INDICATORS

Previous Work

Furnace corrosion problems can be difficult to diagnose and address. However, computational simulations can provide insight into the factors controlling the nature of the flow, temperature, and composition fields within a boiler. Two-phase, reacting, computational fluid dynamics software can simulate boilers fitted with advanced low-NO_x firing systems and provide a detailed description of conditions affecting waterwall corrosion such as local hydrogen sulfide concentration, heat flux, etc. Although the model cannot predict corrosion directly, empirical correlations relating corrosion rates to predicted properties are available. REI has performed computational simulations of several T-, wall- and cyclone-fired units with the goal of understanding and addressing corrosion difficulties related to combustion modifications for the reduction of NO_x emissions. Units evaluated include both subcritical and supercritical units.

The dominant mechanisms of corrosion at locations within a given boiler and from boiler to boiler can vary. Recent studies of corrosion in coal-fired boilers [Nava and Plumley, 1997; EPRI, 1998; Bakker et al., 1999] indicate that corrosion rates can be dominated by the presence of rich gases (H_2S and CO) or by the deposition of coal/char/ash containing unreacted material (sulfur and carbon). Although gas-phase reactions can be important in pulverized-coal-fired boilers, it is thought that the highest corrosion rates encountered (>20 mils/yr) are caused by the deposition of incompletely reacted coal [Davis et al., 1999; EPRI, 1999].

Two recent case studies of supercritical furnaces, one tangentially fired and the other wall fired [Valentine et al., 2000], reinforce the idea that that deposition of sulfur-containing material can lead to extremely high waterwall wastage rates. In CFD simulations of both furnaces, predictions of the locations of high sulfur deposition can be used along with recently developed correlations to identify locations and rates of severe waterwall wastage. Figure 1 presents a comparison between predicted

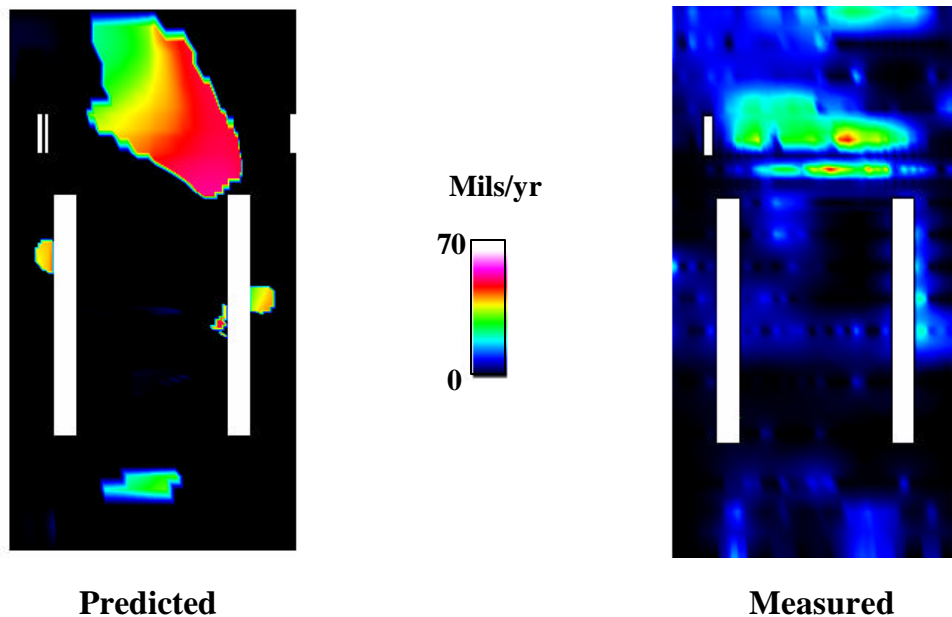


Figure 1. Prediction of Waterwall Corrosion Rates in a Coal-fired Boiler.

corrosion rates due to pyrite deposition and actual measurements of waterwall wastage. The input conditions for utility furnace models vary substantially and are often highly uncertain. In addition, there are a number of additional mechanisms by which waterwall tube material is removed. Given these limitations, the accuracy of the prediction in terms of the rate and location of the high corrosion region is remarkable.

Modeling the Evolution of Included Sulfur

The accuracy of the modeling results for the tangentially fired furnace used in the example above is not impacted significantly by the quality of the prediction of included sulfur arriving at the wall in part because more than 80% of the sulfur in the fuel is contained within excluded pyrite. In addition this excluded pyrite material has an unusually coarse grind (i.e., is composed of large particles). Preliminary studies of other boilers show that it can be difficult to simulate corrosion if the fuel contains a significant fraction of included sulfur. As a first step in addressing this issue, the objective of this effort is to improve our understanding of the evolution of included sulfur, from both pyritic and organic forms. Figure 2 [Vorres, 1990] illustrates the importance of the two forms. The importance of the organic sulfur is often magnified by the fact that much of the pyrite is often excluded.

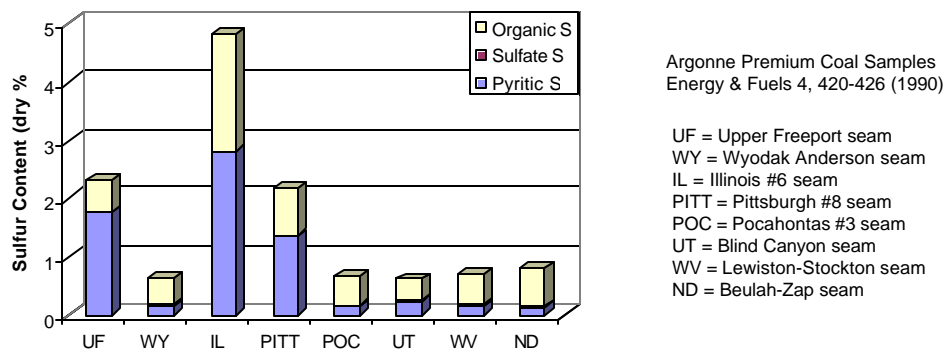


Figure 2. Sulfur distribution for a range of US Coals.

Boal et al. considered included sulfur in a study of the partitioning of iron during pulverized coal combustion. During coal pyrolysis, it was assumed that the pyrite decomposed as if it were excluded. However, the effect of the highly reducing environment within the coal particle can potentially enhance the decomposition [Attar, 1978]. A recent temperature programmed desorption study showed that not only does the coal matrix affect the rate and final decomposition product, but the sulfur released by the pyrite can also interact with the organic matrix [Gryglewicz et al., 1996], which can complicate interpretation of results.

Pyrolysis of the inorganic sulfur forms further complicates the issue. For most coals, it is thought that sulfur is more likely to occur in aliphatic form than other common heteroatoms [Winans et al., 1995]. However, a limited amount of data is currently available for the evaluation of sulfur yields under pyrolysis conditions relevant to coal combustion. Sandia National Labs collected data on sulfur release during pyrolysis and char oxidation for several coals [Mitchell et al., 1992; Fletcher and Hardesty, 1992]. However, since the sulfur data are quite scattered and the uncertainties in the measurement are large, these data provide little evidence to support preferential release of sulfur during pyrolysis.

As with pyrolysis, the evolution of included sulfur during char oxidation is not straightforward. Two issues complicate the situation:

- The penetration of oxygen to the liquid pyritic material within the coal matrix

- The oxidation of sulfur within the organic matrix

Neither of these issues has been explored in satisfactory detail. Bool and coworkers [1995] assumed that the char particle was burning in a diffusion limited manner (regime III) and that the pyrite would oxidize at a rate identical to that of excluded pyrite as it was exposed by the receding surface. This model of char combustion however, is not generally applicable to the combustion of pulverized coal and the validation of the overall model iron partitioning provided little evidence of the accuracy of this submodel. McLennan and coworkers [2000] have performed experiments indicating that the oxidation of the pyrite is retarded by the presence of the organic matrix as evidenced by the high concentration of FeS in Fe-O-S ash particles from the combustion of a coal with a high pyrite concentration.

Given the complexity of the pyrolysis and oxidation processes involved, a detailed model of included sulfur evolution, which would distinguish the behavior of pyrite as well as aromatic and aliphatic forms of organic sulfur, will not be addressed. The purpose of this work is to improve the understanding of bulk sulfur release and to determine coal specific parameters for a three coals of interest.

EXPERIMENTAL

Fuel Selection

Data from three coals will be evaluated, with two of the three from utility plants with severe corrosion problems. Coal A is a common eastern bituminous coal, while coals B and C are high sulfur eastern and midwestern bituminous coals respectively. All coals were received after milling at the plant and were subsequently sieved to a -125 to +45 size fraction. This removes most of the excluded pyrite. Proximate and specific sulfur analyses were also performed and relevant properties are listed in Table 1.

Table 1. Analyses of Coal Samples.

Coal ID	Fixed C/ Volatiles	Moisture	Ash	Sulfur Content	pyritic/ organic
A	2.05	1.4	6.9	2.3	0.8
B	1.29	3.2	6.2	3.1	0.6 [†]
C	1.28	8.9	9.1	3.5	0.4

[†] organic sulfur by difference

Coals B and C have a very similar volatility and sulfur content, while coal A is less volatile and has a lower sulfur content (although still relatively high). The relative amount of pyrite decreases alphabetically.

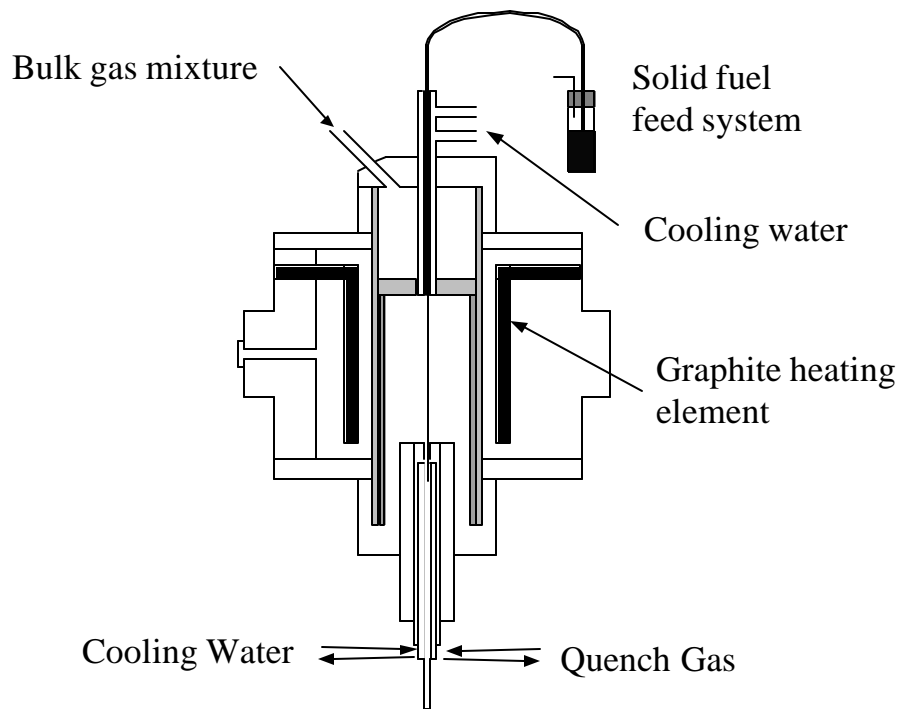


Figure 3. Drop tube furnace for pyrolysis and oxidation experiments.

Apparatus

Pyrolysis and oxidation experiments were performed on the three coals in the high temperature drop tube system illustrated schematically in Figure 3. The system includes the following elements:

- Pneumatic feed system capable of accurate control over a range of 0.1 to 5 g/hr.
- Tube furnace with graphite heating element and cooling system allowing drop tube temperatures up to 1750 K
- Rapid inert quenched, water cooled, sampling probe
- Various particle filtration systems capable of size characterization down to the submicron range
- On-line FTIR spectrometer for gas analysis

Pyrolysis experiments were performed in nitrogen at 1700 K. Oxidation experiments were performed at 1700 K in 6 and 12 percent oxygen (balance nitrogen). Numerical simulations were performed to estimate sample probe locations resulting in approximately 20, 40 and 60% burnout for the char oxidation experiments.

RESULTS

Pyrolysis

The evolution of sulfur during pyrolysis of the three test coals is summarized in Table 2.

Table 2. Volatile yield and sulfur evolution.

Coal ID	% Volatilized	?S/?Mass	Pyritic Sulfur Loss	Organic Sulfur Loss
A	47	1.38	83%	51%
B	62	1.11	90%	57%
C	62	1.13	64%	73%

The volatile yields of the coals are in line with expected values. The lowest yield is for coal A, which had the higher fixed carbon/volatile ratio in Table 1, and coals B and C resulted in nearly identical volatile yields. All of the volatile yields are near ½, as is typical for pulverized coal exposed to high temperatures and high heating rates. Conversely, the sulfur yields are quite surprising. The bulk ratio of the sulfur loss to total mass loss is slightly higher than 1.0 for coals B and C, but significantly higher than 1.0 for coal A. One might expect this effect to be a result of aliphatically bonded organic sulfur, since pyritic decomposition for excluded pyrite would result in sulfur yields between 43 and 50 percent for decomposition to pyrrhotite ($\text{Fe}_{0.877}\text{S}$) or troilite ($\text{Fe}_{1.0}\text{S}$) respectively. However, the opposite is in fact the case. The organic sulfur in coals A and B is released at a rate very similar to that of the remaining organic material and the pyritic material is released in extremely high proportions.

Oxidation

The chars produced in the pyrolysis tests were subsequently reinjected and exposed to oxidizing environments containing 6 and 12 percent oxygen. The partially oxidized chars were then collected at residence times that were selected to result in a range of burnout extents (ideally 20, 40 and 60%). The residence times varied from about 100 to 1000 msec. Figure 4 presents the results of these tests for the 6% oxygen environment. Note that the first data point in each plot is the base point from the pyrolysis tests.

In contrast to the pyrolysis results, the most notable feature of the oxidation results is the extent to which the carbon and the total/pyritic/organic sulfur evolve at virtually identical rates for coals A and C. The pyritic data for coal B do not appear to follow this trend. However, upon closer examination the reliability of this pyritic sulfur data is questionable since the first point indicates a larger amount of pyritic material than existed in the fresh char. Figure 5 shows similar results for the 12% oxygen environment.

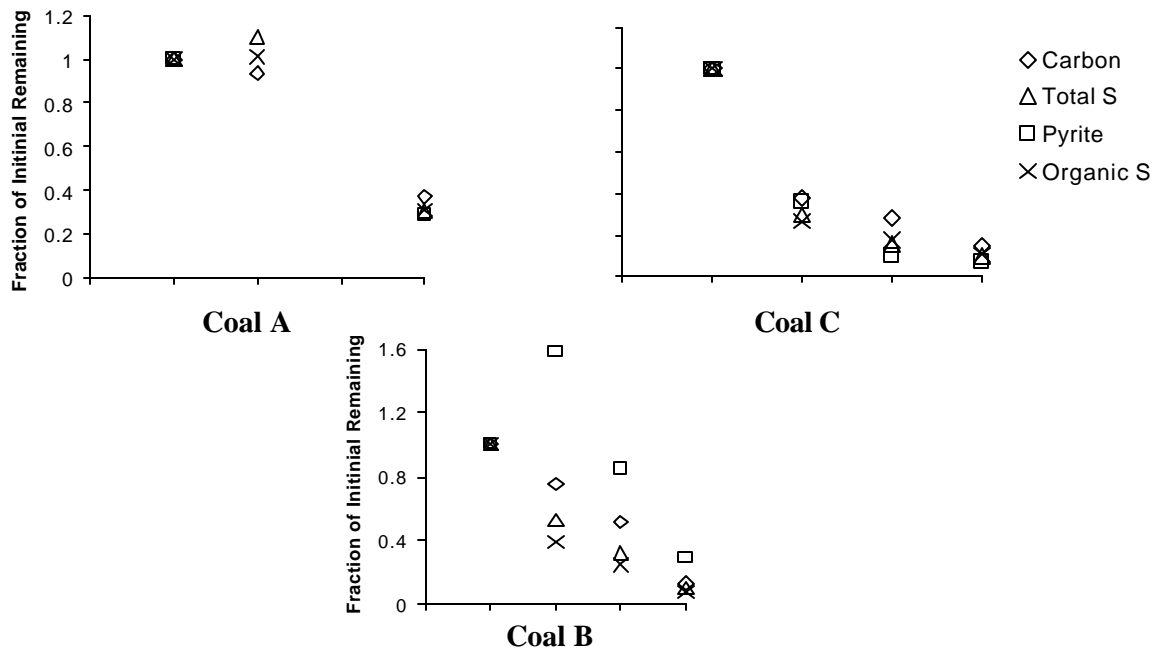


Figure 4. Carbon, total sulfur, pyritic sulfur and organic sulfur retention during the oxidation of coal char with 6% O₂.

CONCLUSIONS

A detailed evaluation of the evolution of sulfur forms during the combustion of three pulverized coals

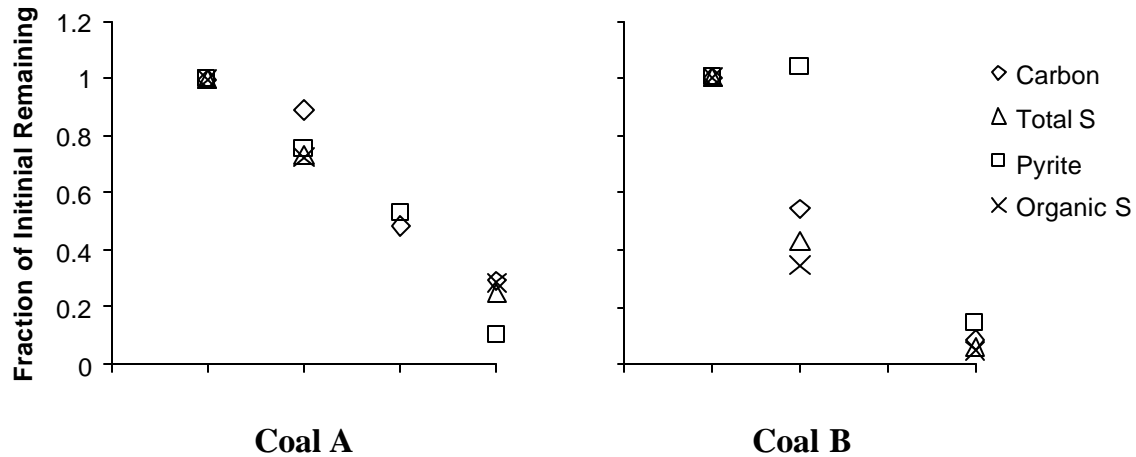


Figure 5. Carbon, total sulfur, pyritic sulfur and organic sulfur retention during the oxidation of coal char with 12% O₂.

illustrates that a more careful consideration of the behavior of included sulfur is necessary. Although this sample set is quite limited, the following approaches to the development of an initial model for the evolution of included pyritic and organic sulfur appear warranted for these specific coals:

- The thermal decomposition of pyritic sulfur is coal specific and, under the reducing conditions within a coal particle, the amount of sulfur released has been observed to exceed that which would result from decomposition of pyrite to troilite (Fe_{1.0}S). A predictive correlation will require a broader range of coals and further study.
- Pyrolysis of organic sulfur appears to be similar to that of the remaining organic structure.
- During char oxidation, total sulfur evolves at a rate similar to that of the remaining organic structure.

REFERENCES

Adams, B., K. Davis, M. Heap, A. Sarofim, G. Eltringham and A. Shook "Application of a reacting CFD model to drop tube kinetics and smelter simulations," Fluid Flow Phenomena in Metals Processing, ed. N. El-Kaddah, The Metallurgical Society: Warrendale, PA, (1999).

Asaki, Z. S. Mori, M. Ikeda and Y. Kondo "Oxidation of pyrrhotite particles falling through a vertical tube," Metallurgical Transactions B: 16B:627 (1985).

Attar, A. Fuel 57:201 (1978).

Bakker, W., S. Kung, M. Heap, J. Valentine "Waterwall corrosion in low NO_x boilers: Root causes and remedies," EPRI-DOE-EPA Combined Utility Air Pollution Control Symposium: The MEGA Symposium, Atlanta, GA, August 16-20, 1999.

Bool, L., T. Peterson and J. Wendt "The partitioning of iron during the combustion of pulverized coal," *Combustion and Flame* 100:262 (1995).

Davis, K., J. Valentine, E. Eddings, M. Heap, W. Bakker, A. Facchiano "Waterwall corrosion after combustion modifications for NO_x control," 24th International Technical Conference on Coal Utilization & Fuel Systems, Clearwater, FL, March 1999.

EPRI Report TR-111152, *Effect of Iron Sulfide on Furnace Wall Corrosion*, Palo Alto, CA: 1998.

Fletcher, T. and D. Hardesty, *Compilation of Sandia Coal Devolatilization Data: Milestone Report, SAND92-8209 · UC-362*, June 1992.

Groves, S., J. Williamson and A. Sanyal "Decomposition of pyrite during pulverized coal combustion," *Fuel* 66:461 (1987).

Gryglewicz, G., P. Wilk, J. Yperman, D. Franco, I. Maes, J. Mullens and L. Poucke "Interaction of the organic matrix with pyrite during pyrolysis of a high-sulfur bituminous coal," *Fuel* 75:1499 (1996).

Huffman, G., Huggins, Levasseur, Chow, Srinivasachar and A. Mehta "Investigation of the transformations of pyrite in a drop-tube furnace," *Fuel* 68:485 (1989).

Jones, C., "Maladies of low-NO_x firing come home to roost," *Power*, Vol. 141, No. 1, p. 54, (1997).

McLennan, A., G. Bryant, B. Stanmore and T. Wall "Ash Formation Mechanisms during pf Combustion in Reducing Conditions," *Energy & Fuels* 14: 150 (2000).

Mitchell, R., R. Hurt, L. Baxter and D. Hardesty, *Compilation of Sandia Coal Char Combustion Data and Kinetic Analyses: Milestone Report, SAND92-8208 · UC-361*, June 1992.

Nava, J. C., A. L. Plumley, and R. Knodler "Wastage control in low emission boiler systems," *Proceedings: Third Int'l Conference on Boiler Tube Failures in Fossil Plants*, Nov. 11-13, 1997.

Srinivasachar, S. and A. Boni "A kinetic model for pyrite transformations in a combustion environment," *Fuel* 68:829 (1989).

ten Brink, H., S. Eenkhoorn, and G. Hamburg "A fundamental investigation of the flame kinetics of coal pyrite," *Fuel* 75: 945 (1996).

Valentine, J., K. Davis, B. Adams, M. Heap, W. Bakker, A. Facchiano "Effect of coal sulfur characteristics on predicted furnace waterwall wastage," *Effects Of Coal Quality On Power Plant Management: Ash Problems, Management and Solutions*, United Engineering Foundation, May 8 - 11, 2000, Park City, Utah.

Vorres, K.S., "The Argonne Premium Coal Sample Program," *Energy and Fuels* 5:420 (1990).

Winans, R., Y. Kim, J. Hunt and R. McBeth "Structural elucidation of Argonne premium coals: molecular weights, heteroatom distributions and linkages between clusters," *Proc. Int. Conf. Coal Science*, Oviedo, Spain, 1271-1274, 1995.

ACKNOWLEDGEMENTS

This work is funded by EPRI under the supervision of Wate Bakker and Tony Facchiano. The technical contributions of Dana Overacker and Alejandro Molina at the University of Utah are greatly appreciated